# Relaxation of an unstable state in parametrically excited cold atoms

Geol Moon,[1] Yonghee Kim,[1] Myoung-Sun Heo,[1] Jina Park,[1] Dahyun Yum,[1] Wanhee Lee,[1]
Heung-Ryoul Noh,[2] and Wonho Jhe[1,*]

[1]*Department of Physics and Astronomy, Seoul National University, Seoul 151-747, Korea*
[2]*Department of Physics, Chonnam National University, Gwangju 500-757, Korea*

(Received 24 June 2011; revised manuscript received 21 August 2011; published 30 September 2011)

We investigate the scaling behavior of the relaxation process for an unstable state near a subcritical Hopf bifurcation point. When the parametric modulation is applied to a magneto-optical trap, the atomic cloud becomes unstable and decays to the dynamic bistable states. Near the subcritical Hopf bifurcation point, we experimentally show that the relaxation process exhibits the scaling behavior; the relaxation time shows a scaling exponent of $-1.002$ ($\pm 0.024$). We also present the passage time distribution for the statistical interpretation of the escape process associated with the relaxation of the unstable state. We compare the experimental results to the numerical and analytic results, demonstrating the good agreement between them.

DOI: 10.1103/PhysRevE.84.036217 PACS number(s): 05.45.−a, 37.10.Gh, 05.70.Ln

## I. INTRODUCTION

The relaxation process of a macroscopic system that is initially prepared in an unstable state is an intriguing problem in nonequilibrium physics [1], as it is related to such areas as transient-laser radiation [2–5], spinodal decomposition [6,7], superfluorescence [8–10], and hydrodynamic instabilities [11]. Theoretical research in this area has been performed from various perspectives [2,12–16].

One of the characteristics of the relaxation process for an unstable state in those studies is the scaling behavior. In particular, the relaxation dynamics near the bifurcation point shows the scaling behavior, and the scaling exponent depends on the nature of the initial state and the type of instability involved. There have been many studies of the relaxation dynamics in various nonlinear systems exhibiting the bifurcation dynamics, such as the saddle-node bifurcation, pitchfork bifurcation, and supercritical Hopf bifurcation [17]. However, it has been an experimental challenge to study the relaxation dynamics near the subcritical Hopf bifurcation point due to its difficult experimental accessibility [18–20].

In the parametrically modulated magneto-optical trap (MOT), which is an ideal model system for such a study due to its intrinsic nonlinear and stochastic nature, phenomena such as the parametric resonance, Hopf bifurcation [21,22], and a noise-induced transition between two phase-space attractors [23] are observed. Moreover, the many-body nature of the MOT exhibits the time-translational symmetry breaking as well as the ideal mean-field phase transition [24,25]. In the parametrically excited atomic system, one can consider two attractors in the phase space as a dynamic double well, where the midpoint between the two wells is apparently an unstable state. This study takes into account the relaxation process from an unstable state near the subcritical Hopf bifurcation point in nonlinear dynamics. In this paper, we investigate the relaxation of an unstable state near the bifurcation point where the unstable state becomes stable. First, we measured the relaxation time of the atomic population in the unstable state. Its relaxation asymptotically shows the exponential behavior. Over an extended period, this exponential relaxation time was observed to diverge in a manner inversely proportional to the distance from the bifurcation point. Second, we measured the passage time distribution, which provides the complementary information about the relaxation process, at the boundary in the phase space midway between the unstable and stable state [26,27]. The results show that it takes more time to reach the dynamic stable state as the bifurcation point is approached. The numerical simulation and analytic calculation are in good agreement with the experimental results.

The paper is organized as follows: In Sec. II, we demonstrate the theoretical approach of the dynamics of the unstable state near the bifurcation point. To this we apply a proper approximation, leading to the analytic form of the decay in the center of a cloud. In Sec. III, the experimental results are presented and compared to the theoretical results. Section IV summarizes the results.

## II. THEORY

The trapped atomic motion inside a MOT is approximately described by a damped harmonic oscillator with a nonlinear term, as follows [22]:

$$\ddot{z} + \beta\dot{z} + \omega_0^2 z + A_0\,\omega_0^2 z^3 = f(t), \tag{1}$$

Here, $\beta$ is the damping coefficient, $\omega_0$ is the trap frequency, and $A_0$ is the nonlinear coefficient of the MOT. In addition, $f(t)$ denotes the random force that originates from the spontaneous emission, and $\langle f(t)f(t')\rangle = 2D\delta(t-t')$. Here $D = \beta k_B T/m$ represents the Doppler diffusion, where $m$ is the mass of atom, $k_B$ is the Boltzmann constant, and $T$ is the temperature of the atom. We experimentally measure the decay of atomic population at the trap center where the nonlinear term is negligible, and therefore the stationary distribution of the atomic cloud near $(z,v) = (0,0)$ in the phase space approximately has a Gaussian form

$$\rho_0(z,v) = \frac{\beta\omega_0}{2\pi D}\exp\left[-\beta\left(\omega_0^2 z^2 + v^2\right)/2D\right]. \tag{2}$$

As $\omega_0^2$ is modulated by $\omega_0^2[1+\epsilon\cos(\omega_F t)]$, where $\epsilon$ is the modulation amplitude and $\omega_F$ is modulation frequency, it gives rise to parametric excitation where the parametric modulation

*whjhe@snu.ac.kr

 ©2011 American Physical Society

frequency is nearly twice the trap frequency. The atomic population occupies a bistable state after the departure from its initial state, as described in Eq. (2). The atomic motion is described in a rotating frame using the standard procedure of an averaging method [25,28] with slowly varying variables $X$ and $Y$, as follows:

$$z(t) = C\left[X\cos\left(\frac{\omega_F t}{2}\right) - Y\sin\left(\frac{\omega_F t}{2}\right)\right],$$
$$\dot{z}(t) = -C\frac{\omega_F}{2}\left[X\sin\left(\frac{\omega_F t}{2}\right) + Y\cos\left(\frac{\omega_F t}{2}\right)\right], \quad (3)$$

where $C = (2\epsilon/3A_0)^{1/2}$. Then the atomic motion of Eq. (1) in this frame is

$$\frac{dX}{d\tau} = -\frac{1}{\zeta}X + Y[1+\mu-(X^2+Y^2)] + \xi_1(\tau),$$
$$\frac{dY}{d\tau} = -\frac{1}{\zeta}Y + X[1-\mu+(X^2+Y^2)] + \xi_2(\tau), \quad (4)$$

where $\xi_1(\tau)$ and $\xi_2(\tau)$ are independent random forces [28]. The dimensionless time $\tau$ and dimensionless parameters $\zeta$ and $\mu$ are given by

$$\tau = \frac{\epsilon\omega_0^2}{2\omega_F}t, \quad \zeta = \frac{\epsilon\omega_0^2}{\omega_F\beta}, \quad \mu = \frac{\omega_F^2 - 2\omega_F\omega_0}{2\epsilon\omega_0^2}. \quad (5)$$

In this paper, we focus on the relaxation process from the unstable equilibrium point $(X_{\rm eq}, Y_{\rm eq}) = (0,0)$. Near the subcritical bifurcation point $\mu \approx \mu_B = \sqrt{1-1/\zeta^2}$, one direction of the motion of the system becomes slower than the other direction. Using the center manifold theorem [29], we can separate the fast variable$P$ and slow variable $Q$ by applying an additional coordinate transform, as follows [28]:

$$P = X\cos\varphi - Y\sin\varphi, \quad Q = X\sin\varphi + Y\cos\varphi, \quad (6)$$

where $\varphi = \frac{1}{2}\arcsin(1/\zeta)$. In this frame, Eq. (4) has the form

$$\frac{dP}{d\tau} = -2\zeta^{-1}P + Q[\mu_B + \mu - (P^2+Q^2)] + \xi_P(\tau),$$
$$\frac{dQ}{d\tau} = P[\mu_B - \mu + (P^2+Q^2)] + \xi_Q(\tau). \quad (7)$$

The fast variable $P$ reaches its quasistationary value $P \approx \zeta\mu_B Q$ with the dimensionless relaxation time $\zeta/2$. On the other hand, the slow variable $Q$ has a relaxation time which goes to infinity. Therefore, the fast variable $P$ follows adiabatically the slow variable $Q$, and we can neglect the noise term in the equation of $P$. This finally gives the one-dimensional (1D) equation of motion for the slow variable $Q$, as follows:

$$\dot{Q} = \zeta\mu_B\eta Q + \zeta^3\mu_B Q^3 + \xi(\tau), \quad (8)$$

where $\eta = \mu_B - \mu$, and $\xi(\tau)$ is the noise with properly scaled intensity $D_0$. We consider that for the near subcritical bifurcation point, the parameter $\eta$ satisfies $0 < \eta \ll 1$.

We can calculate the many stochastic trajectories of Eq. (7) numerically as shown in Fig. 1. From the numerical calculation data, we extract the passage time distribution (PTD). The overall behaviors are very similar to the experimental one as shown in Fig. 4(a). We will explain this in more detail in Sec III.

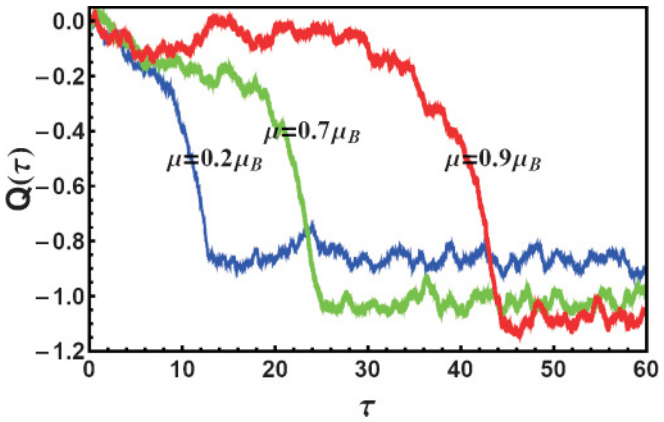


FIG. 1. (Color online) Typical stochastic trajectories obtained from a numerical simulation with the initial condition of $Q(0) = 0$ for different values of $\mu$. We adopt $D_0 = 0.5$ and $\zeta = 1.275$. The larger $\mu$ indicates the closer distance from the bifurcation point $\mu_B$ where the characteristic slowing down become manifest.

The time evolution of the system is one-dimensional, and we can easily describe the time evolution of the density distribution of the atomic cloud using the Fokker-Planck equation and directly compare it to the experimental data. The corresponding Fokker-Planck equation of Eq. (8) is

$$\frac{\partial\rho}{\partial\tau} = -\frac{\partial}{\partial Q}[(\zeta\mu_B\eta Q + \zeta^3\mu_B Q^3)\rho] + D_0\frac{\partial^2\rho}{\partial Q^2}. \quad (9)$$

The initial condition is the distribution of Eq. (2), and transforming this initial distribution into the new frame gives

$$\rho(Q,\tau=0) = (2\pi\zeta D_0)^{-1/2}\exp(-Q^2/2\zeta D_0). \quad (10)$$

The above equation is easily solved in the restricted region, where $Q^2 \ll \eta\zeta^{-2}$, implying that the nonlinear term is negligible. In this regime, we can obtain the solution of Eq. (9) with Eq. (10), as follows:

$$\rho(Q,\tau) = \sqrt{\frac{\lambda}{2\pi D_0\sigma(\tau)}}\exp[-\lambda Q^2/2D_0\sigma(\tau)], \quad (11)$$

Here, $\lambda = \zeta\mu_B\eta$ and $\sigma(\tau) = (1+\lambda\zeta)e^{2\lambda\tau} - 1$.

The time evolution of the distribution at the trap center, $\rho(Q=0,\tau)$, is initially in a nonexponential form; however, at a dimensionless time that satisfies $\exp(2\lambda\tau) \gg 1$, it shows exponential decay behavior, as follows:

$$\rho(Q=0,\tau) \approx \sqrt{\frac{\lambda}{2\pi D_0(1+\zeta\lambda)}}\exp(-\lambda\tau). \quad (12)$$

The asymptotic relaxation time $\tau_r$ demonstrates scaling behavior, which is inversely proportional to the distance from the bifurcation point.

$$\tau_r = 1/\lambda \propto (\mu_B - \mu)^{-1}. \quad (13)$$

The scaling exponent is $-1$.

## III. EXPERIMENTAL RESULTS AND DISCUSSIONS

The unstable state forms at the trap center by parametrically driving the trapped atomic cloud at the proper modulation

frequency and amplitude. Our experimental setup is the typical six-beam MOT of $^{85}$Rb where one pair of trapping lasers counterpropagating along the anti-Helmholtz coil axis is intensity-modulated, resulting in parametric resonance as shown in Fig. 2 [22–24]. The sinusoidal signal generated by the function generator is fed into acousto-optic modulator, which modulates the trap laser beam. The magnetic field gradient $b$ is 0.11 T/m, the modulation amplitude of the trap laser $\epsilon$ is 0.8, and the saturation parameter $s_0$ and detuning $\delta$ are 0.2 and $-2.55\ \Gamma$, respectively. $\Gamma$ is the decay rate of the excited state ($=2\pi \times 6.07$ MHz).

In our system, we observed the limit cycles (i.e., phase-space orbit attractors) and supercritical and subcritical Hopf bifurcation varying modulation frequency $\omega_F$ [22]. Below the subcritical bifurcation point, the unstable state is placed at the trap center, and stable states are located at the point where the two clouds are fully apart. To observe the escape of the

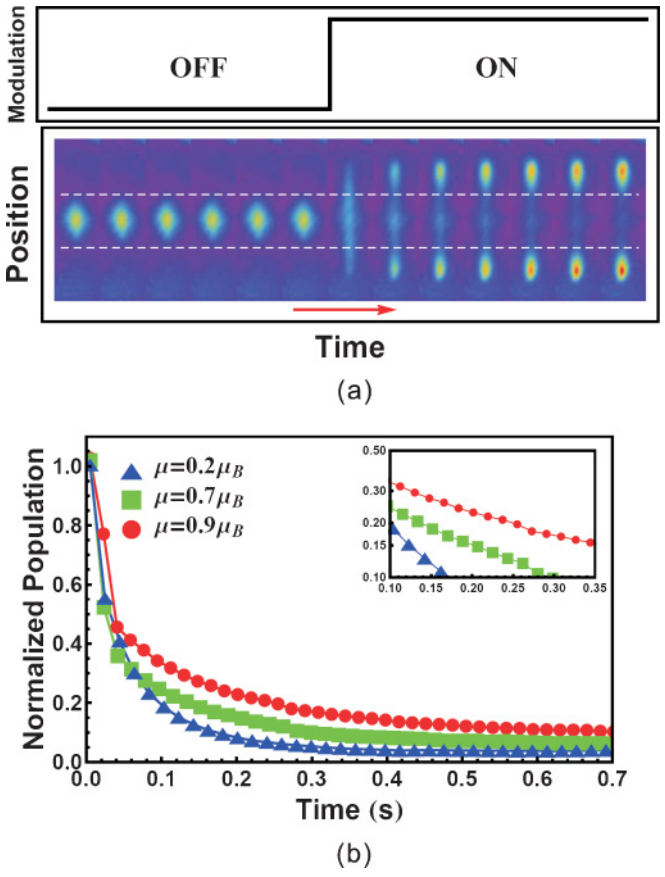


FIG. 2. (Color online) Typical procedure to measure the temporal change of atomic population. (a) The time sequence of the relaxation of the unstable state (central atomic cloud) is shown after the modulation is turned on. The 2D images of atomic population are obtained by charge-coupled device (CCD) detection at a time interval of 0.02s. The oscillatory atomic motion is periodically observed to be specifically timed, in which two outermost clouds are fully apart. (b) The typical decay of the atomic population for the unstable cloud is shown from the experimental results. The critical slowing down effect is manifest as the bifurcation point is approached from the blue to the red line in sequence; the slope in the inset (semi-log plot) represents the decay rate λ and the more bifurcation point is close, the more slope is gentle.

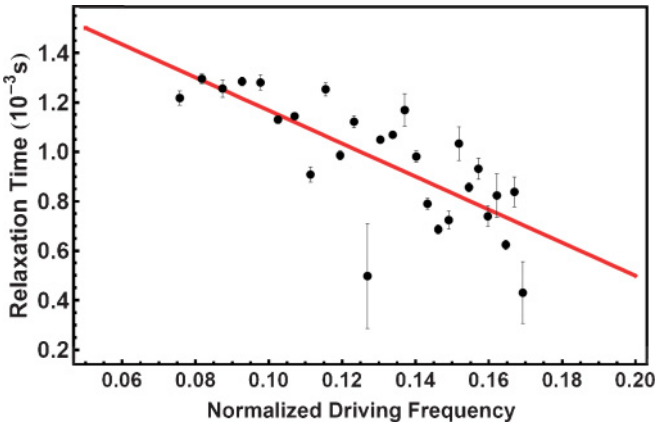


FIG. 3. (Color online) Scaling behavior of the relaxation process from the unstable state. The relaxation time increases exponentially as it approaches the bifurcation point, and the scaling exponent is $-1.002$ ($\pm 0.024$) (log-log plot). The error bars show the standard deviation for the fitting error.

atomic population from the unstable state, we started by putting atoms at the trap center without modulation of the intensity, after which we suddenly turned on the intensity modulation. In such a situation, the trap center becomes unstable and atoms begin to wash away from the center as time passes, as seen in Fig. 2(a). Figure 2(b) experimentally displays the typical decay of the normalized atomic population at the center of the atomic cloud at a different distance from the bifurcation point. We can obtain the relaxation time from its asymptotic exponential curve.

Figure 3 displays the relaxation time of the atomic population in an unstable state versus the normalized driving frequency rescaled by $(\omega_B - \omega_F)/\omega_B$ experimentally. $\omega_B - \omega_F$ is proportional to $\mu_B - \mu$, and approaching the measured bifurcation point, $\omega_B (= 113.5$ Hz), it shows the power-law behavior of the relaxation time, as expected from Eq. (13). The measured scaling exponent is $-1.002$ ($\pm 0.024$). Physically, this means that the system stays longer in an unstable state as the modulation frequency $\omega_F$ moves closer to the bifurcation point $\omega_B$. In Fig. 1, the trajectories obtained from a numerical simulation clearly show this feature. Such a slowing down effect of relaxation can also be rephrased in terms of the passage time distribution as follows.

As shown in Fig. 4, in addition to the relaxation time from the unstable state, we also considered the passage time distribution (PTD) experimentally (a) and theoretically (b). The PTD is defined by probability distribution $P(t)$ that a particle arrives at an arbitrary given boundary in the phase space (or real space) at time $t$ after starting from its unstable state.

PTD can be directly obtained by measuring the atomic population at a given coordinate value with time. The chosen coordinate for the measurement should be located where the process has clearly escaped from the unstable state. Here, we chose a value between the unstable and stable state [white dashed line in Fig. 2(a)]. Figure 4 shows the probability $P(\tau)$ that the particle reaches the coordinate at the dimensionless time $\tau$. It is clear that the PTD has a longer tail due to the late departure of the particle from an

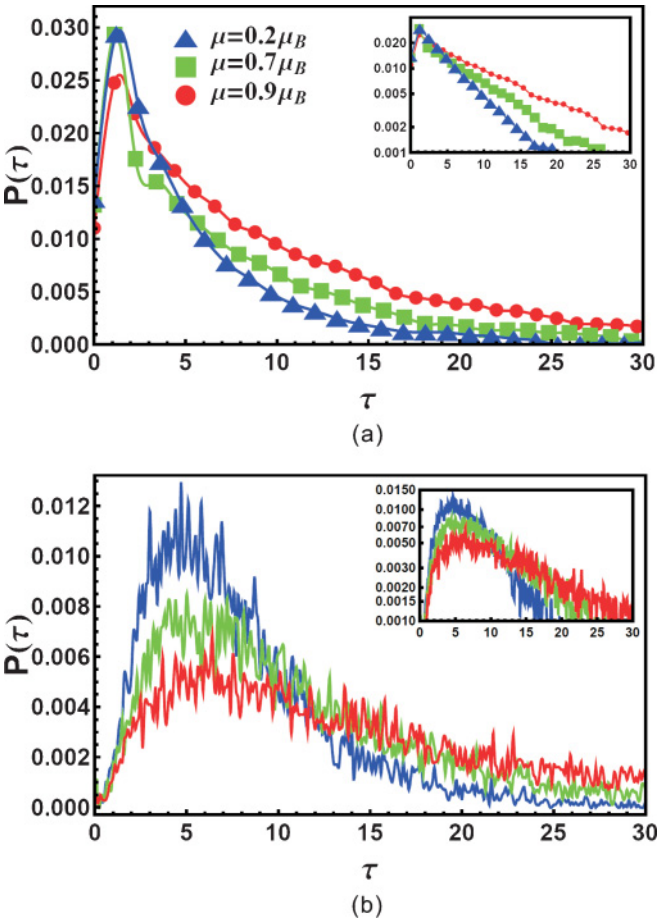


FIG. 4. (Color online) Passage time distribution of the system: (a) experiment, (b) numerical simulation. The scaled noise intensity $D_0$ is 0.5 and $\zeta$ is 1.275 in (a) and (b). Blue, green, and red lines denote $\mu = 0.2\mu_B$, $0.7\mu_B$, and $0.9\mu_B$, respectively. The slope in the inset (semi-log plot) clearly shows that the closer the bifurcation point is, the later particles in the unstable state arrive at the boundary.

unstable state as the bifurcation point becomes approached closer. The experimental results are qualitatively in good agreement with the simulation results. However, there is quantitative disagreement where the time distribution value $P(\tau)$ in Fig. 4(a) is larger than that in Fig. 4(b). The reason is because the tail of the Gaussian-distributed atomic cloud in a stable state experimentally remains at the boundary, after which the value of the time distribution increases. Moreover, the time distribution of atoms that move from the stable state to the unstable state due to a noise-induced transition, which is not considered in the simulation, enhances the value of the time distribution. As another cause, the coefficients in Eq. (1) derived from the one-dimensional MOT equation are different from those observed experimentally, as reported in an earlier study [30]. This would also bring about the quantitative difference.

## IV. CONCLUSION

We have discussed the relaxation process from an unstable state near the subcritical Hopf bifurcation point generated by a parametrically excited MOT. The relaxation time at the unstable point was observed to diverge due to the slowing down of the escape process as the bifurcation point was approached. The relaxation time showed a power-law dependence on the distance from the bifurcation point with a the scaling exponent of $-1.002$ ($\pm 0.024$), which is in good agreement with theoretical results. We also discussed the complementary passage time distribution and provided a qualitative explanation of the statistical characteristics for the escape process. The present study may deepen our understanding of the general relaxation process of the unstable state in a nonequilibrium nonlinear dynamical system and its scaling behaviors.

## ACKNOWLEDGMENTS

We would like to thank M. I. Dykman for useful discussions. This work was supported by the Acceleration Research Program of the Korean Ministry of Science and Technology. G.M. was supported by a Korea Student Aid Foundation (KOSAF) grant funded by the government of Korea (MEST Grant No. S2-2009-000-01627-1).

[1] H. Haken, *Synergetics* (Springer, Berlin, 1977).
[2] F. Haake, Phys. Rev. Lett. **41**, 1685 (1978).
[3] M. Suzuki, J. Stat. Phys. **16**, 477 (1977).
[4] F. T. Arecchi and V. Degiorgio, Phys. Rev. A **3**, 1108 (1971).
[5] F. T. Arecchi, V. Degiorgio, and B. Querzola, Phys. Rev. Lett. **19**, 1168 (1967).
[6] J. S. Langer, M. Baron, and H. D. Miller, Phys. Rev. A **11**, 1417 (1975).
[7] K. Kawasaki, M. C. Yalabik, and J. D. Gunton, Phys. Rev. A **17**, 455 (1978).
[8] F. Haake, H. King, G. Schröder, J. Haus, R. Glauber, and F. Hopf, Phys. Rev. Lett. **42**, 1740 (1979).
[9] F. Haake, J. Haus, H. King, G. Schröder, and R. Glauber, Phys. Rev. Lett. **45**, 558 (1980).
[10] D. Polder, M. F. H. Schuurmans, and Q. H. F. Vrehen, Phys. Rev. A **19**, 1192 (1979).
[11] A. C. Newell, and J. A. Whitehead, J. Fluid Mech. **38**, 279 (1969).
[12] H. Risken and H. D. Vollmer, Z. Phys. **204**, 240 (1967).
[13] B. Caroli, C. Caroli, and B. Roulet, J. Stat. Phys. **21**, 415 (1979).
[14] F. T. Arecchi and A. Politi, Phys. Rev. Lett. **45**, 1219 (1980).
[15] M. Suzuki, J. Stat. Phys. **16**, 11 (1977).
[16] F. de Pasquale, P. Tartaglia, and P. Tombesi, Phys. Rev. A **25**, 466 (1982).
[17] S. H. Strogatz, *Nonlinear Dynamics and Chaos* (Westview, Cambridge, 2000).
[18] R. Holzner, B. Derighetti, M. Ravani, and E. Brun, Phys. Rev. A **36**, 1280 (1987).
[19] A. Baugher, P. Hammack, and J. Lin, Phys. Rev. A **39**, 1549 (1989).
[20] Laurent Larger and Jean-Pierre Goedgebuer, Phys. Rev. E **69**, 036210 (2004).

[21] K. Kim, H.-R. Noh, Y.-H. Yeon, and W. Jhe, Phys. Rev. A **68**, 031403 (2003).
[22] K. Kim, H.-R. Noh, and W. Jhe, Opt. Commun. **236**, 349 (2004).
[23] K. Kim, M.-S. Heo, K.-H. Lee, H.-J. Ha, K. Jang, H.-R. Noh, and W. Jhe, Phys. Rev. A **72**, 053402 (2005).
[24] K. Kim, M.-S. Heo, K.-H. Lee, K. Jang, H.-R. Noh, D. Kim, and W. Jhe, Phys. Rev. Lett. **96**, 150601 (2006).
[25] M.-S. Heo, Y. Kim, K. Kim, G. Moon, J. Lee, H.-R. Noh, M. I. Dykman, and W. Jhe, Phys. Rev. E **82**, 031134 (2010).
[26] P. Colet, F. De Pasquale, M. O. Cáceres, and M. San Miguel, Phys. Rev. A **41**, 1901 (1990).
[27] F. Haake, J. W. Haus, and R. Glauber, Phys. Rev. A **23**, 3255 (1981).
[28] M. I. Dykman, C. M. Maloney, V. N. Smelyanskiy, and M. Silverstein, Phys. Rev. E **57**, 5202 (1998).
[29] J. Guckenheimer and P. Holmes, *Nonlinear Oscillators, Dynamical Systems and Bifurcations of Vector Fields* (Springer-Verlag, New York, 1987).
[30] G. Moon, M. S. Heo, Y. Kim, H. R. Noh, D. Kim, and W. Jhe, Phys. Rev. A **81**, 033425 (2010).